Electrochemically Controllable Conjugation of Proteins on Surfaces

Paula M. Mendes,*[,†,||] Karen L. Christman,[†] Puru Parthasarathy,[‡] Eric Schopf,[‡] Jianyong Ouyang,[§] Yang Yang,[§] Jon A. Preece,[⊥] Heather D. Maynard,[†] Yong Chen,[‡] and J. Fraser Stoddart*[,†]

California NanoSystems Institute and Department of Chemistry and Biochemistry, Department of Mechanical and Aerospace Engineering, and Department of Materials Science and Engineering, University of California, Los Angeles, 405 Hilgard Avenue, Los Angeles, CA 90095-1569 and Department of Chemical Engineering, and School of Chemistry, The University of Birmingham, Edgbaston, Birmingham, B15 2TT, U.K. Received June 21, 2007; Revised Manuscript Received September 5, 2007

The rational design of surfaces for immobilization of proteins is essential to a variety of biological and medical applications ranging from molecular diagnostics to advanced platforms for fundamental studies of molecular and cell biology. We have developed an advanced electrochemically based approach for site-selective and reaction-controlled immobilization of proteins on surfaces. When a molecular monolayer of 4-nitrothiophenol on gold electrode surfaces is reduced electrochemically in a selective fashion at its nitro groups, to afford amino groups by potentiometric scans, the amine can be employed to orchestrate the immobilization of proteins to the surface. This protein immobilization strategy could allow one to fabricate intricate protein structures on surfaces for addressing fundamental and applied problems in biology and medicine.

INTRODUCTION

The controlled immobilization of proteins on surfaces is of paramount importance for a wide variety of applications, ranging from the development of model substrates for mechanistic studies of cell behavior to high-throughput protein assays for drug discovery, clinical diagnostics, and proteomics (*1–7*). In particular, stimulated by the success of DNA arrays in genomics (*1*), substantial scientific and commercial interest has been generated in the use of protein arrays as tools for proteomics (*1, 2*). However, proteins are much more chemically and structurally diverse than nucleic acids, making them intrinsically more complicated to be immobilized on surfaces (*1, 2*). Other difficulties result from the intrinsic fragility of proteins, which have modest conformational stability and can be damaged upon surface immobilization (*1, 2*). Moreover, proteins can adhere and adsorb to most surfaces through a variety of mechanisms (electrostatic interaction, hydrogen bonding, hydrophobic interactions, and/or a combination of these), resulting in nonspecific protein binding (*8*).

Therefore, a primary enabling technology is the ability of controlling the immobilization of proteins on surfaces while avoiding nonspecific protein binding and retaining protein native biological features and properties (*1–3, 5–7*). Molecular surface science has greatly contributed to the advancement of this technology by providing ideal platforms for bioengineering surfaces on a molecular level (*9–15*). For instance, self-assembled monolayers (SAMs), which form spontaneously by the adsorption of an active surfactant onto a solid surface, possess important properties of self-organization and adaptability to a number of technologically relevant surface substrates. The properties of a SAM (thickness, structure, surface energy, stability) can be easily controlled, and specific functionalities can also be introduced into the building blocks. For instance, SAMs of thiols on gold and triethoxysilanes on silicon dioxide (SiO_2) have been exploited (*6, 8, 16–18*) to provide the surfaces not only with active groups that interact with specific moieties of the protein to be immobilized, but also with protein-resistant groups such as poly(ethylene glycol) (PEG).

Proteins have been immobilized onto these surfaces by either adsorption of the proteins (*8*), molecular recognition between the proteins and immobilized ligands (*19*), or covalent coupling to the SAM surface (*16, 17*). The most common conjugation methods rely on the covalent attachment of proteins to "static" (*20*) surfaces chemically modified with different protein-reactive groups, including activated esters (*16*), aldehydes (*21*), or maleimides (*22–24*). On the other hand, strategies for "turning-on" protein reactive groups at SAM surfaces by an "on demand" surface reaction using an external stimulus have great potential as versatile platforms for protein immobilization. Similar strategies have been employed to immobilize urease onto a polymer film (*25*), as well as other biomolecules, such as DNA (*26*) and peptides (*27, 28*) on SAM surfaces, yet protein immobilization onto a SAM using this "on demand" surface reaction approach has not been previously demonstrated.

Here, we report an approach to control protein immobilization on surfaces based on SAMs that can switch from bio-inert to bioactive states in response to an applied electrical potential. The approach we have developed is based on an electrochemical reaction in which aromatic nitro (NO_2) groups, self-assembled on gold surfaces, can be chemically modified by a redox process to amino (NH_2) groups, which can then be used to orchestrate the immobilization of the proteins. Our strategy involves (Figure 1) five steps: (1) functionalization of the electrically addressable gold surfaces with NO_2-terminated SAMs; (2) spatially selective electrochemical reduction (*26, 29–31*) of the NO_2 groups

* Correspondence addresses: Dr. Paula M. Mendes, Department of Chemical Engineering, University of Birmingham, Edgbaston, Birmingham, B15 2TT (UK), Tel: Int. code +(121) 414-5343, Email: p.m.mendes@bham.ac.uk. Dr. J. Fraser Stoddart, Department of Chemistry and Biochemistry, University of California, Los Angeles, 405 Hilgard Avenue, Los Angeles, CA 90095-1569 (USA), Tel: Int. code +(310) 206-7078, Email: stoddart@chem.ucla.edu.

[†] California NanoSystems Institute and Department of Chemistry and Biochemistry, University of California, Los Angeles.

[‡] California NanoSystems Institute and Department of Mechanical and Aerospace Engineering, University of California, Los Angeles.

[§] California NanoSystems Institute and Department of Materials Science and Engineering, University of California, Los Angeles.

[⊥] School of Chemistry, The University of Birmingham.

[||] Present address: Department of Chemical Engineering, The University of Birmingham.

10.1021/bc7002296 CCC: $37.00
Published on Web 10/26/2007

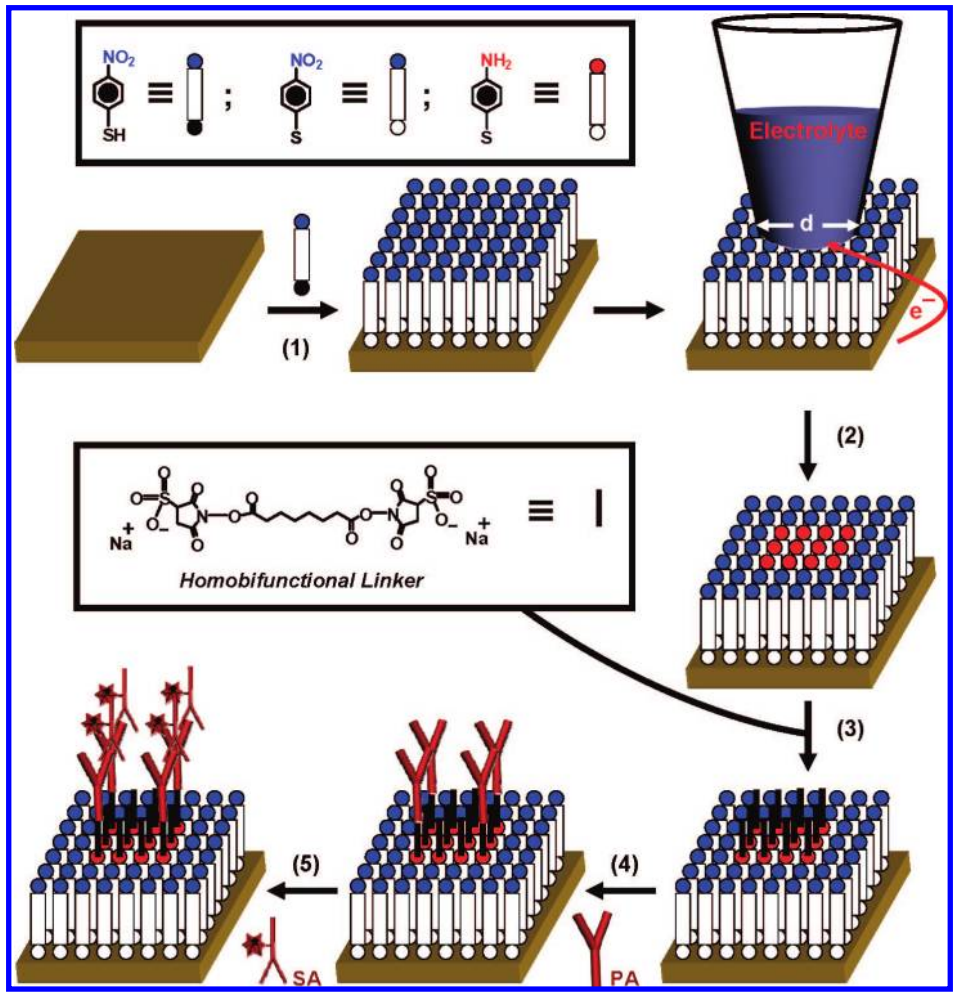

Figure 1. Schematic illustration of the electrochemical conversion from a NO_2 group in the SAMs of 4-nitrothiophenol on an Au electrode to an NH_2 group, which is capable of subsequently inducing the immobilization of primary antibodies, PA (red). Bound primary antibodies are detected using fluorescently labeled secondary antibodies, SA (red). The electrochemical reduction is conducted selectively on the Au electrode area exposed to the electrolyte (diameter (d) = 8 mm).

to primary NH_2 groups; (3) selective reaction of the resulting NH_2-terminated monolayers with a homobifunctional linker; (4) covalent immobilization of primary antibodies; (5) visualization of these bound primary antibodies using fluorescently labeled secondary antibodies. Fluorescence microscopy and surface plasmon resonance (SPR) spectroscopy were employed to characterize the immobilization of antibodies and their selective assembly to the modified areas of the SAM.

EXPERIMENTAL PROCEDURES

SAM Preparation. Substrates with 30 nm thick Au employing a 10 nm thick Ti adhesion layer on an n-type Si wafer were fabricated by electron-beam evaporation. The Au substrates were cleaned with piranha solution (3:1, H_2SO_4/30% H_2O_2), rinsed with ultra high purity (UHP) H_2O (resistivity = 18 MΩ cm) and then HPLC-grade EtOH thoroughly for 1 min. (*Caution: Piranha solution reacts violently with all organic compounds and should be handled with care*). Subsequently, the substrates were immersed in a 0.1 mM ethanolic solution of 4-nitrothiophenol (Sigma-Aldrich) for 12 h to form the SAMs on the Au surfaces. The substrates were rinsed with EtOH and UHP H_2O.

Electrochemical Conversion. The cyclic voltammograms (CVs) of the NO_2-terminated SAMs and their conversion on the Au electrodes were performed using a Princeton Applied Research VMP multichannel potentiostat with a custom-designed Teflon cell, equipped with the functionalized Au substrate as the working electrode, a Pt wire as the counter electrode, and the standard calomel electrode (SCE) as the reference electrode. The planar gold working electrode exposes a circular geometric area of 50 mm^2 to the electrolyte solution. Cyclic voltammetry was carried out at a scan rate of 200 mV/s.

Protein Immobilization. The pristine 4-nitrothiophenol and converted 4-nitrothiophenol SAMs were incubated with a 5 mg/mL solution of bis(sulfosuccinimidyl)suberate (BS^3; Pierce) in phosphate buffered saline pH 7.4 (PBS) for 20 min at room temperature. Samples were rinsed with PBS (~1 min) and incubated with a primary mouse anti-human vascular endothelial growth factor (VEGF) antibody (Biosource) with a concentration of 25 μg/mL in PBS containing 0.1% Triton X-100 (PBS–Triton) for 20 min. The samples were rinsed in PBS buffer solution for 10 min and incubated in the dark for 20 min in a 20 μg/mL PBS–Triton solution of Alexa Fluor 568 goat anti-mouse IgG antibody (Molecular Probes). The substrates were rinsed with PBS for 10 min and mounted for fluorescence microscopy. For the control samples, the pristine 4-nitrothiophenol and converted 4-nitrothiophenol SAMs were stained as described above, without first immobilizing the BS^3 homobifunctional linker.

X-ray Photoelectron Spectroscopy (XPS). XPS experiments were performed in an Omicron XPS/UPS system using a monochromatic Al K_α X-ray source (1486.6 eV) with a pass energy of 50 eV. Fitting of XPS peaks was performed using the *Avantage v2.2* processing software. All spectra were fitted using 30% Lorentzian/70% Gaussian peaks.

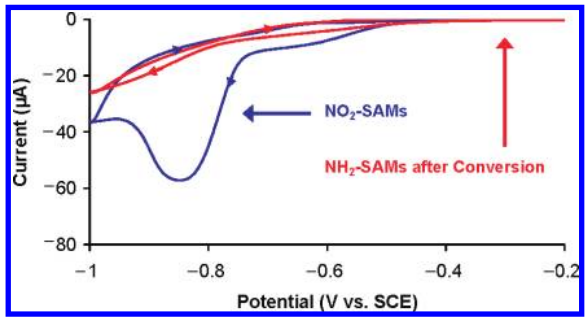

Figure 2. CV (blue curve) of a SAM of 4-nitrothiophenol—the reduction of NO_2 to NH_2 groups appears as a pronounced peak at around −0.85 V. CV (red curve) of the SAM of 4-nitrothiophenol after the reductive scan.

Fluorescence Microscopy. Fluorescence images were collected on a Zeiss Axiovert 200 fluorescent microscope, equipped with an AxioCam MRm monochrome camera. Pictures were acquired using AxioVision LE 4.1 with identical exposure parameters and analyzed using *Image J 1.33u* (NIH). No postexposure image processing was performed.

Surface Plasmon Resonance. SPR spectroscopy experiments were performed with a Biacore X at 25 °C at a flow rate of 2 μL/min. Two different monolayers—pristine 4-nitrothiophenol and converted 4-nitrothiophenol—were prepared on Biacore gold sensor chips. Prior to protein binding studies, 40 μL of a 5 mg/mL solution of the BS^3 homobifunctional linker in PBS, was injected into the gold sensor, followed by a PBS–Triton washing for 10 min. The functionalized gold surfaces (either pristine or converted) were subsequently exposed to a primary antibody by injection of 40 μL of anti-streptavidin produced in rabbit (Sigma) at a concentration of 1.4 mg/mL in PBS–Triton. The protein solution was replaced with the PBS–Triton solution for 25 min to remove any unbound primary antibody. Subsequently, a 40 μL sample of the secondary antibody, Alexa Fluor 488 goat anti-rabbit IgG (Molecular Probes), with a concentration of 20 μg/mL in PBS–Triton was injected, followed by a 10 min PBS–Triton washing.

RESULTS

Cyclic voltammetry (CV) was used to investigate the characteristics of the SAMs and for the chemical conversion ($NO_2 \rightarrow NH_2$) on the gold surfaces. The CV study of the NO_2-terminated SAMs was carried out in three subsequent CV scans. A 0.1 M KCl solution (9:1, EtOH/UHP H_2O) (*26*) was employed as the electrolyte to check the characteristic CV peak that the NO_2 group exhibits (blue curve in Figure 2) (*29*). Next, a second scan was carried out in a 0.1 M KCl aqueous solution to ensure (*29*) an adequate supply of H^+ ions for the complete electrochemical reduction of the NO_2 to NH_2 groups. Finally, the disappearance of the NO_2 group-related peak was observed by running a third scan (red curve in Figure 2) in a 0.1 M KCl solution (9:1, EtOH/UHP H_2O). The potential was swept from 0 to −1.0 V with respect to the SCE. The reductive peak of the NO_2 group was observed at −0.85 V (blue curve in Figure 2). By integrating the area under the reductive peak, the SAMs density was found to be 2.6×10^{14} molecule/cm^2. After the reduction of the NO_2 groups during the second scan, no redox activity was observed (red curve in Figure 2), implying complete conversion of the NO_2-terminated SAMs.

High-resolution XPS spectra were acquired on the gold electrodes before and after surface electrochemical modification. XPS measurements confirmed the conversion of the NO_2 groups (N(1s) binding energy = 405.6 eV; blue curve in Figure 3) to the NH_2 counterparts (N(1s) binding energy = 399.6 eV; red curve in Figure 3). XPS of the pristine 4-nitrothiophenol surfaces also indicated the presence of primary amines. This behavior can be attributed (*32, 33*) to the gradual reduction of the NO_2 groups to NH_2 groups (Figure 3; blue curve) during X-ray irradiation initiated by the photoelectrons and secondary electrons emitted from the surface. However, in the electrochemically converted NO_2-terminated SAM, the XPS of the N(1s) binding energy region indicated only the presence of the NH_2 group with a strong peak at 399.6 eV.

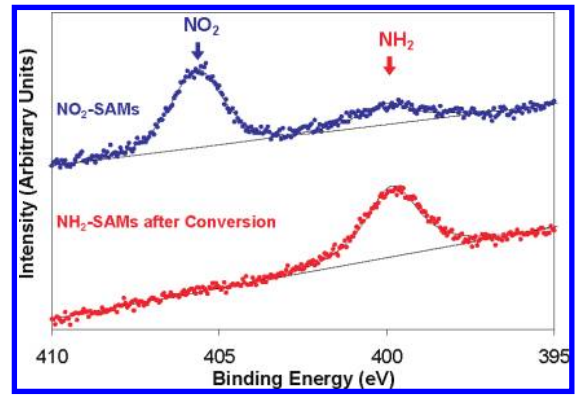

Figure 3. XPS spectra of the N(1s) peak region of a SAM of 4-nitrothiophenol before (blue curve) and after (red curve) the reductive scan. The binding energy of the N (1s) has been shifted by 6 eV, which is consistent with a reduction of NO_2 to NH_2 groups.

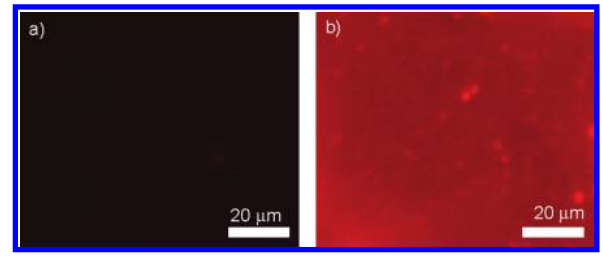

Figure 4. Fluorescence microscope images of a (a) nonconverted and (b) converted NO_2-terminated monolayer region after being sequentially exposed to BS^3, a primary antibody, and a red fluorescent Alexa Fluor 568 conjugated secondary antibody.

Following the XPS confirmation of the efficient electrochemical reduction, the viability of this strategy for the site-selective assembly of proteins on gold surfaces was demonstrated first by fluorescence microscopy. After performing electrochemical conversion on large-scale electrodes (converted area: 50 mm^2 on a 1 cm^2 gold surface area), the electrochemically generated NH_2 groups were activated with the BS^3 homobifunctional linkers to expose amine-reactive *N*-hydroxysulfosuccinimide (Sulfo-NHS) groups. Subsequently, the primary mouse anti-human VEGF antibody was allowed to react with the modified gold surface, followed by incubation with a red fluorescent secondary antibody. Detection of the binding of the primary antibodies to the electrochemically modified surfaces was evaluated by fluorescence microscopy. Figure 4a,4b illustrates the fluorescence microscope images collected from the NO_2- and NH_2-terminated regions of the surface, respectively. The fluorescence images of the regions terminated by the amino groups (Figure 4b) clearly revealed high fluorescence intensity, while the unmodified areas (NO_2 groups) showed minimal fluorescence. The signal-to-noise ratio (specific binding on NH_2-terminated regions/nonspecific binding on NO_2-terminated regions) was determined to be 26, a ratio which demonstrates the high degree of biological specificity to the NH_2 surface over the NO_2 surface.

Control experiments were also established to verify that the selective immobilization of proteins on the NH_2-terminated regions relied on the formation of amide bonds first between

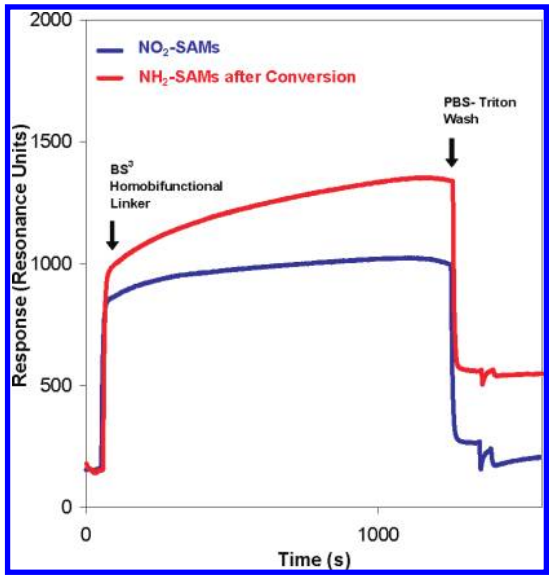

Figure 5. SPR sensorgram traces for the immobilization of BS^3 homobifunctional linker on a SAM of 4-nitrothiophenol (blue curve) and 4-nitrothiophenol after the reductive scan (red curve). SPR spectroscopy data show the selective immobilization of BS^3 to the converted NO_2-terminated monolayers.

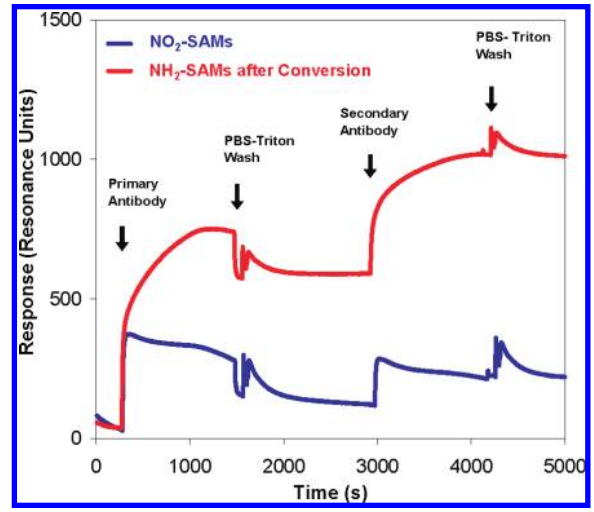

Figure 6. SPR sensorgram traces for the sequential immobilization of a primary antibody followed by a secondary antibody on a SAM of 4-nitrothiophenol (blue curve) and 4-nitrothiophenol after the reductive scan (red curve). The surfaces were washed with PBS–Triton after each protein injection. The antibodies show high binding affinity for converted NO_2-terminated monolayers, whereas negligible antibody adsorption is noted on nonconverted NO_2-terminated monolayers.

the BS^3 homobifunctional linker and the amino groups on the surface, and subsequently between the BS^3 homobifunctional linker and the primary amine groups in the primary antibody. For instance, in the absence of immobilization of the BS^3 homobifunctional linker on the nonconverted and converted NO_2-terminated monolayers, no protein immobilization occurred and no fluorescence was observed. Further evidence of the covalent immobilization of BS^3 on the NH_2 monolayers was obtained by surface plasmon resonance spectroscopy. Nonconverted and converted NO_2-terminated monolayers were exposed to a BS^3 linker solution and their immobilization monitored by SPR (Figure 5). BS^3 was shown to bind irreversibly to the converted NO_2-terminated monolayers, whereas no immobilization was observed for the NO_2-terminated monolayers.

A large SPR response was also observed upon introducing the primary rabbit anti-streptavidin antibody to the NH_2 monolayers activated with succinimidyl esters (Figure 6). When PBS buffer was passed through the system for approximately 30 min, essentially no protein desorbed from the converted monolayer surface. These data establish that the proteins are not nonspecifically adsorbed on the gold surface and thus are likely covalently attached to the surface via the BS^3 linker. These results contrasted with the negligible nonspecific protein binding on pristine NO_2-terminated monolayers, particularly after washing with PBS. Indeed, the protein surface coverage was determined (*34*) to be 56 ng/cm^2 for the NH_2 monolayer regions compared to 8 ng/cm^2 on the pristine NO_2 monolayer regions. The primary antibody immobilized on the NH_2 monolayers was subsequently recognized by the secondary antibody, leading to another sharp increase in the SPR response. After injection of the secondary antibody, the irreversible nature of the protein binding was confirmed by the steady SPR response, following PBS–Triton washing for 10 min. SPR spectroscopy showed that the irreversible immobilization of protein was specific for NH_2 monolayers, and that the pristine NO_2 monolayers effectively prevented unwanted nonspecific binding. This feature is particularly important for binding multiple proteins to a single substrate via the electrochemical activation described herein.

CONCLUDING REMARKS

The NO_2-terminated groups in the SAMs of 4-nitrothiophenol on gold surfaces can be reduced electrochemically and selectively to NH_2 groups by applying a negative voltage between the addressed electrode and its counter electrode in the presence of an electrolyte. By employing the homobifunctional activated ester linker, proteins can then be attached specifically to the NH_2 monolayer region. We have demonstrated that immobilized antibodies exhibit high affinity and selectivity for these NH_2 regions, after activation, as monitored by fluorescence microscopy and surface plasmon resonance spectroscopy. This strategy can potentially be extended to immobilize sequentially a series of different proteins onto selected gold nanoelectrodes by carrying out repeated cycles with the entirely aqueous solution-based, and hence biocompatible, electrochemical and protein immobilization processes. Efforts in this direction are underway.

ACKNOWLEDGMENT

The authors acknowledge support of this work through a Nanoscale Interdisciplinary Research Team (NIRT) Grant (0404458) and through SINAM (DMI-0327077) from the National Science Foundation. KLC would like to thank the NIH NHLBI for a NRSA Postdoctoral Fellowship. JAP would like to thank the European Community for support (NANO3D.NMP-CT-2005-014006).

LITERATURE CITED

(1) Niemeyer, C. M., and Mirkin, C. A. (2004), Wiley-VCH Verlag GmbH & Co. KGaA, Weinheim.
(2) Kambhampati, D. (2004), Wiley-VCH Verlag GmbH & Co. KGaA, Weinheim.
(3) Cui, Y., Wei, Q. Q., Park, H. K., and Lieber, C. M. (2001) Nanowire nanosensors for highly sensitive and selective detection of biological and chemical species. *Science 293*, 1289–1292.
(4) Zheng, G. F., Patolsky, F., Cui, Y., Wang, W. U., and Lieber, C. M. (2005) Multiplexed electrical detection of cancer markers with nanowire sensor arrays. *Nat. Biotechnol. 23*, 1294–1301.
(5) Shekhawat, G., Tark, S. H., and Dravid, V. P. (2006) MOSFET-embedded microcantilevers for measuring deflection in biomolecular sensors. *Science 311*, 1592–1595.
(6) Christman, K. L., Enriquez-Rios, V. D., and Maynard, H. D. (2006) Nanopatterning proteins and peptides. *Soft Matter 2*, 928–939.

(7) Demidov, V. V. (2004) Nanobiosensors and molecular diagnostics: a promising partnership. *Expert Rev. Mol. Diagn. 4*, 267–268.
(8) Mrksich, M. (2005) *MRS Bull. 30*, 180–184.
(9) Sagiv, J. (1980) Organized monolayers by adsorption.1. formation and structure of oleophobic mixed monolayers on solid-surfaces. *J. Am. Chem. Soc. 102*, 92–98.
(10) Maoz, R., and Sagiv, J. (1984) On the formation and structure of self-assembling monolayers.1. a comparative ATR-wettability study of Langmuir-Blodgett and adsorbed films on flat substrates and glass microbeads. *J. Colloid Interface Sci. 100*, 465–496.
(11) Gun, J., Iscovici, R., and Sagiv, J. (1984) On the formation and structure of self-assembling monolayers.2. a comparative-study of Langmuir-Blodgett and adsorbed films using ellipsometry and IR reflection absorption-spectroscopy. *J. Colloid Interface Sci. 101*, 201–213.
(12) Netzer, L., and Sagiv, J. (1983) A new approach to construction of artificial monolayer assemblies. *J. Am. Chem. Soc. 105*, 674–676.
(13) Netzer, L., Iscovici, R., and Sagiv, J. (1983) Adsorbed monolayers versus Langmuir-Blodgett monolayers - why and how.1. from monolayer to multilayer, by adsorption. *J. Am. Chem. Soc. 99*, 235–241.
(14) Nuzzo, R. G., and Allara, D. L. (1983) Adsorption of bifunctional organic disulfides on gold surfaces. *J. Am. Chem. Soc. 105*, 4481–4483.
(15) Mendes, P. M., and Preece, J. A. (2004) Precision chemical engineering: integrating nanolithography and nanoassembly. *Curr. Opin. Colloid Interface Sci. 9*, 236–248.
(16) Lee, S. W., Oh, B. K., Sanedrin, R. G., Salaita, K., Fujigaya, T., and Mirkin, C. A. (2006) Biologically active protein nanoarrays generated using parallel dip-pen nanolithography. *Adv. Mater. 18*, 1133–1136.
(17) Lee, K. B., Park, S. J., Mirkin, C. A., Smith, J. C., and Mrksich, M. (2002) Protein nanoarrays generated by dip-pen nanolithography. *Science 295*, 1702–1705.
(18) Mrksich, M. (2002) What can surface chemistry do for cell biology? *Curr. Opin. Chem. Biol. 6*, 794–797.
(19) Hyun, J., Ahn, S. J., Lee, W. K., Chilkoti, A., and Zauscher, S. (2002) Molecular recognition-mediated fabrication of protein nanostructures by dip-pen lithography. *Nano Lett. 2*, 1203–1207.
(20) Choi, I. S., and Chi, Y. S. (2006) Surface reactions on demand: electrochemical control of SAM-based reactions. *Angew. Chem., Int. Ed. 45*, 4894–4897.
(21) Christman, K. L., and Maynard, H. D. (2005) Protein micropatterns using a pH-responsive polymer and light. *Langmuir 21*, 8389–8393.
(22) Jung, H., Kulkarni, R., and Collier, C. P. (2003) Dip-pen nanolithography of reactive alkoxysilanes on glass. *J. Am. Chem. Soc. 125*, 12096–12097.
(23) Cheung, C. L., Camero, J. A., Woods, B. W., Li, T., Johnson, J. E., and De Yoreo, J. J. (2003) Fabrication of assembled virus nanostructure on templates of chemoselective linkers formed by scanning probe nanolithography. *J. Am. Chem. Soc. 125*, 6848–6849.
(24) Smith, J. C., Lee, K.-B., Wang, Q., Finn, M. G., Johnson, J. E., Mrksich, M., and Mirkin, C. A. (2003) Nanopatterning the chemospecific immobilization of cowpea mosaic virus capsid. *Nano Lett. 3*, 883–886.
(25) Hernández, E. C., Witkowski, A., Daunert, S., and Bachas, L. G. (1995) Potentiometric enzyme electrode for urea based on electrochemically prepared polypyrrole membranes. *Mikrochim. Acta 121*, 63–72.
(26) Lee, C. S., Baker, S. E., Marcus, M. S., Yang, W. S., Eriksson, M. A., and Hamers, R. J. (2004) Electrically addressable biomolecular functionalization of carbon nanotube and carbon nanofiber electrodes. *Nano Lett. 4*, 1713–1716.
(27) Yeo, W.-S., and Mrksich, M. (2006) Electroactive self-assembled monolayers that permit orthogonal control over the adhesion of cells to patterned substrates. *Langmuir 22*, 10816–10820.
(28) Collier, J. H., and Mrksich, M. (2006) Engineering a biospecific communication pathway between cells and electrodes. *Proc. Natl. Acad. Sci. U.S.A. 103*, 2021–2025.
(29) Tsutsumi, H., Furumoto, S., Morita, M., and Matsuda, Y. (1995) Electrochemical-behavior of a 4-nitrothiophenol modified electrode prepared by the self-assembly method. *J. Colloid Interface Sci. 171*, 505–511.
(30) Nielsen, J. U., Esplandiu, M. J., and Kolb, D. M. (2001) 4-Nitrothiophenol SAM on Au(111) investigated by in situ STM, electrochemistry, and XPS. *Langmuir 17*, 3454–3459.
(31) Yang, W. S., Baker, S. E., Butler, J. E., Lee, C. S., Russell, J. N., Shang, L., Sun, B., and Hamers, R. J. (2005) Electrically addressable biomolecular functionalization of conductive nanocrystalline diamond thin films. *Chem. Mater. 17*, 938–940.
(32) Mendes, P., Belloni, M., Ashworth, M., Hardy, C., Nikitin, K., Fitzmaurice, D., Critchley, K., Evans, S., and Preece, J. (2003) A novel example of X-ray-radiation-induced chemical reduction of an aromatic nitro-group-containing thin film on SiO_2 to an aromatic amine film. *ChemPhysChem 4*, 884–889.
(33) Mendes, P. M., Jacke, S., Critchley, K., Plaza, J., Chen, Y., Nikitin, K., Palmer, R. E., Preece, J. A., Evans, S. D., and Fitzmaurice, D. (2004) Gold nanoparticle patterning of silicon wafers using chemical e-beam lithography. *Langmuir 20*, 3766–3768.
(34) Fivash, M., Towler, E. M., and Fisher, R. J. (1998) BIAcore for macromolecular interaction. *Curr. Opin. Biotechnol. 9*, 97–101.

BC7002296